Journal of the European Ceramic Society 19 (1999) 2619–2623

PII: S0955-2219(99)00056-4
0955-2219/99/$ - see front matter

# Arch Effect in High Isostatic Pressure Compacts

I.Yu. Prokhorov

Physico-Technical Institute, R.Luxemburg str. 72, Donetsk 340114, Ukraine

(Received 28 May 1998; accepted 21 February 1999)

***Abstract***

*Arch effect arising under isostatic pressing of the cylindrical or spherical powder compacts is commonly known to cause a loosely packed interior region inside the pressings. Using the results of the shell stability theory it is shown that under definite compact's geometry and powder characteristics, arch effect can involve latent cracking of the pressing as well, with its final breakdown during green machining or sintering. Experiments using 0·6 GPa large alumina pressing revealed all the above phenomena including formation of an overpressed cylindrical layer with predicted 0·133R (R is the radius of the pressing) thickness and close packing density. It is concluded that each CIP route must be pre-calculated as for specified shape, powder and green machining in order to find CIP pressures lower than the critical shell breakdown pressure or higher than the powder's yield stress where the arch effect disappears.* © *1999 Elsevier Science Limited. All rights reserved*

*Keywords*: pressing, shaping, failure analysis, porosity, biomedical applications.

## 1 Introduction

The term 'arch effect' had arisen from construction mechanics where wedged bricks anciently were used to form the arches over openings. Such bridging is known to have a place in granular materials as well. It is known from the powder metallurgy[1,2] that the arch effect arises under CIP of cylindrical or spherical compacts and results in poor working out of the interior regions by external pressure. It is recommended to apply various binders in order to suppress this detrimental phenomenon. Rectangular shapes involve less problems in this respect.

However, in modern ceramic technology, where advanced materials are generally produced from ultrafine powders, application of any binders is often too expensive or unfavourable, whilst most CIP compacts, especially those subjected to green machining, have just cylindrical or spherical shapes or sections.[3] All the above makes studies in conditions and sequences of the arch effect under CIP quite actual.

## 2 Theoretical Considerations

During isostatic compression of a powder, its surface particles wedge between underlying ones and push them apart with forces proportional to the cotangent of the wedge angle. As a consequence, the hydrostatic stress component in the surface layer appears to be *higher* than the applied pressure, and the powder is intensively densified upon quasi-hexagonal close packing (CP) lattice of particles is formed.

A number of theoretical works,[4–6] and many others, in excellent agreement with experiments, give for random close packings a plane coordination number very close to 6 and bulk coordination number close to 12 (for example, 5·92 in ref. 4 and 11·4 in ref. 5 for $\Pi = 0{\cdot}3$). As one can see below,the experimental data (Fig. 4 in comparison with Table 1) show that the green density in surface layer almost coincides with theoretical h.c.p. density for spheres. Therefore, adopted simplified quasi-h.c.p. model in the work is at least reasonable.

As far as mean angle between particles in such a lattice is about 120°, the applied pressure should be transmitted down along a straight chains of particles diverging from each point of surface under the above angle. Such force chains are positioned in the cylindrical layer between circumscribing and inscribing circles around and inside right hexagon in the cross-section [Fig. 1(a)]. One can easily calculate that a thickness ($h$) of such a layer is

$$h = R(1 - \cos 30^\circ) \cong 0{\cdot}133R \qquad (1)$$

where $R$ is the cylinder's radius.

The layer protects the interior from pressing against the applied pressure, and a loosely packed region should be formed inside it.

**Table 1.** Relevant characteristics of ceramic materials under studying

| *Material* | *Composition* | *Young modulus GPa* | *Crystal density, g/cm³* | *Elastic modulus of CP compact, GPa* | *Apparent density of CP compact, g/cm³* |
|---|---|---|---|---|---|
| PSZ | $ZrO_2 + 3$ mol% $Y_2O_3$ | 200 | 6·1 | 120 | 3·4 |
| Alumina | $Al_2O_3 + 0{\cdot}3$ w% MgO | 400 | 4·0 | 240 | 2·2 |

Such a region should arise in rectangular compacts close to cube as well [Fig. 1(b)], but it would be much smaller, about

$$a^* = a(1 - \tan 30^\circ)\cos 30^\circ \cong 0{\cdot}37a \qquad (2)$$

where $a$ is the cube's edge.

Finally, in a long bar the cross section is worked out by pressure practically entirely as in previous case [Fig. 1(c)] while longitudinal sections are worked out much less [Fig. 1(d)]. It is why the shrinkages in longitudinal and cross directions appear considerably different leading to the compact's shape distortion.

Thus, the most important consequences of arch effect should take place in cylindrical or spherical compacts. They result in announced inhomogenuity of properties of sintered ceramic-ware as well as possible shape distortion. Moreover some problems can arise during green machining, in particular, drilling.

Nevertheless, all the above does not include all possible aspects of arch effect in powder compacts. From the mechanical point of view, compacts in Fig. 1 are nothing else but compressed elastic shells which can break on reaching their stability limits. Let us consider stability criteria for the cylindrical shell in this approach.

According to elastic theory,[7] the cylindrical elastic shell with length $L$, radius $R$, wall thickness $h$, elastic modulus $E$, and Poisson's ratio $v$ (which hereafter is considered equal to 0·3) loses its stability at critical external pressure

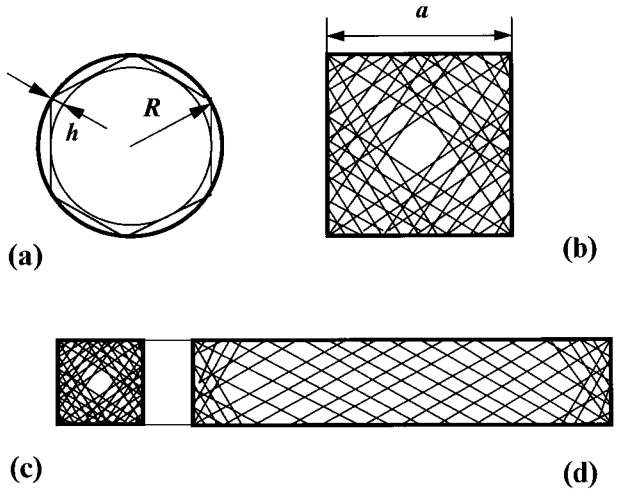


**Fig. 1.** Arch effect patterns in cross-sections of cylinder or ball (a), cube (b) and bar (c,d).

$$p^* = \frac{\sqrt{6}}{9(1 - v^2)^{3/4}} E \left(\frac{h}{R}\right)^{5/2} \frac{\pi R}{L} \qquad (3)$$

by way of distortion with $n$ buckles in cross-section. It is supposed that eqn (3) is valid when the shell is long$(\pi R/nL)^2 << 1$) and thin-walled ($h/R << 1$) as well as a number of buckles

$$n = \sqrt[4]{6\pi^2\sqrt{1 - v^2}} \sqrt{\frac{R}{L}} \sqrt[4]{\frac{R}{h}} \qquad (4)$$

is large enough ($n > 2$).

In the case of a powder compact with specified geometry ($R/L$) its wall thickness ($h/R$) is determined by eqn (1) while elastic modulus $E$ depends on porosity $\Pi$. There exist many works devoted to the calculation of elastic moduli in porous materials.[8] However, all of them give approximately the same estimation of $E$ for presented porosity values in good agreement with cited experiments. It can be noticed that the most of such works relate to *sintered* porous materials where particles cannot move one along another. But isostatically compressed powder under high pressure is rather similar to sintered ceramics because all degrees of freedom therein are already taken out. Elastic moduli of powder pressings *under* high pressure have not been measured yet as far as it is known; besides, it should be made by special (acoustical or so) methods.[9] Using the simplest Knudsen relation[10] one can present the dependence of the modulus on porosity as

$$E = E_0 \exp(-k\Pi) \qquad (5)$$

where $E_0$ is Young's modulus for bulk material, $k$ is a constant characterizing the shape (excentricity) of pores. Since for sintered ceramics with elongated grain boundary pores the value of $k$ usually varies from 4 to 6,[10] for green compacts one obviously should accept a nearly uniaxial shape of spaces between particles with $k \cong 2$. As for the value of $\Pi$, it can be accepted equal to 0·26 for close packing of spherical particles inside the shell. As a result, it follows from eqn (5) that $E \cong 0{\cdot}6E_0$.

In rectangular compacts the problem of shell stability is apparently absent due to large wall thickness, see eqn (2) and Fig. 1(b)–(d).

Finally, for spherical shell with radius $R$ the theory[7] predicts

$$p^* = \frac{2}{\sqrt{3(1-\nu^2)}} E \left(\frac{h}{R}\right)^2 \qquad (6)$$

## 3 Experimental Results

Two most typical ceramic materials had been chosen for studying various aspects of arch effect as having quite different elastic characteristics presented in Table 1.

Ultrafine powders of both materials consist of few micrometre sized granules composed by nanometrical closely packed crystallites. Therefore 'close packing of the powder' in this case implies close packing of granules with resulting density 0·74 by 0·74 equal to 0·56 from the crystal density.

Calcinated press-powders without any binders were preformed into bars 6 by 6 by 42 mm in size in steel pressform and then isostatically pressed using 'wet bag' route in hydrostats. Obtained dependences of green densities and shrinkages on CIP pressure are presented in Fig. 2.

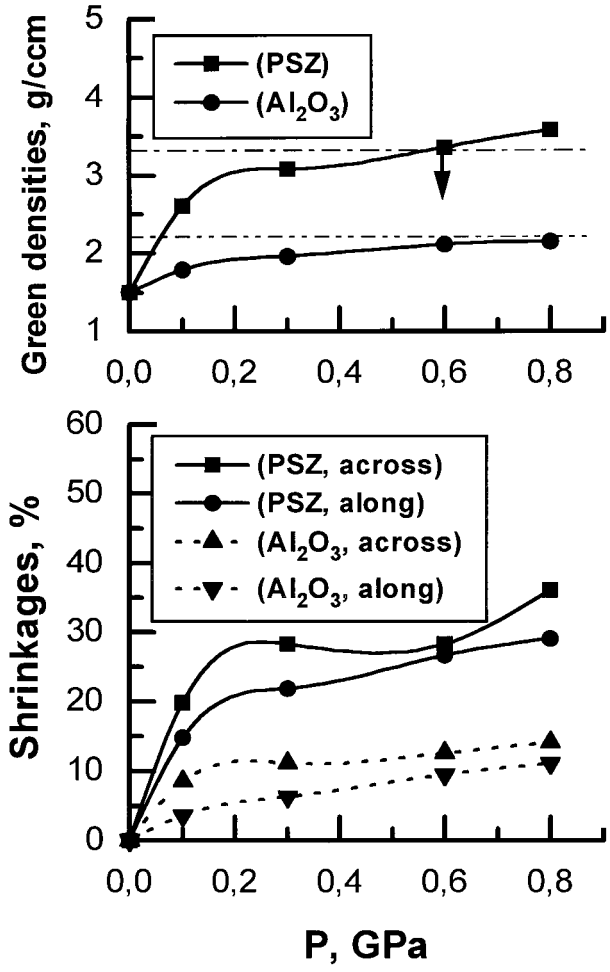


**Fig. 2.** Shrinkages and green densities of rectangular bars made of PSZ and $Al_2O_3$ powders as functions of CIP pressure. Arrow shows close packing (CP) of particles at the beginning of plasticity.

As it can be seen from the figure, cross shrinkages of the bars at lower CIP pressures are markedly higher than longitudinal ones in accordance with arch effect patterns in Fig. 1(c) and (d). Shrinkages become isotropic only at CIP pressure corresponding to close packing and equal to 0·6 GPa for PS2 and about 1·2 GPa for alumina.

Physically, achievement of a close packed state in a powder compact implies that the material becomes homogeneous and hence the arch effect disappears. Naturally it should be related to blurring out the force chains, that in turn can be associated with disturbation of the angles between them. Such disturbation can easily be explained by plastic deformation of powder particles. Indeed, at room temperature yield stress for PSZ is about 0·6 GPa[11] and for $Al_2O_3$ about 1·2 GPa[12] in full compliance with Fig. 2.

It should be noticed that a local plastic deformation have place in the contact regions of powder's particles, in particular, granules, even at quite low pressures.[13] However, such local deformation hardly results in displacements of the particles and hence blurring out the force lines.

To study the arch effect directly the large-scaled $Al_2O_3$ powder compact has been prepared. About 600 g of the press-powder was tamped into thin-walled cylindrical pressform with 96 mm in diameter and 129 mm in height. The pressform was hydrostatically pressed using 'wet bag' route at 0·6 GPa. Self-heating of the compact immediately after CIP was about 70–80°C. An even cylindrical body was obtained after unpacking, with 70 mm in diameter and 94 mm in height; both shrinkages were found to be equal to 27%.

An attempt was made to drill and machine the compact. However, it was discovered during green drilling that the bottom half of the compact is pierced with cracks forming irregular network, with mean block size about 10–30 mm. Thereafter, the compact was crushed down with hammer into pieces 0·5–1·0 g in weight with thorough registration of each piece's position inside the compact. Apparent density of each registered piece was estimated using hydrostatic weighting in water after wax covering; density measurement accuracy, together with scattering (as determined from comparison of values for neighbouring pieces along the same circumference inside the cylinder) were better than 2%.

Obtained data allow the plotting of two dependences of green density on distance, namely, axial along the principal axis of cylinder and radial in top (safe) half of the compact. Axial dependence of green density is presented in Fig. 3. It shows that the material had undergone strong arch effect which is manifested in a loosely packed central

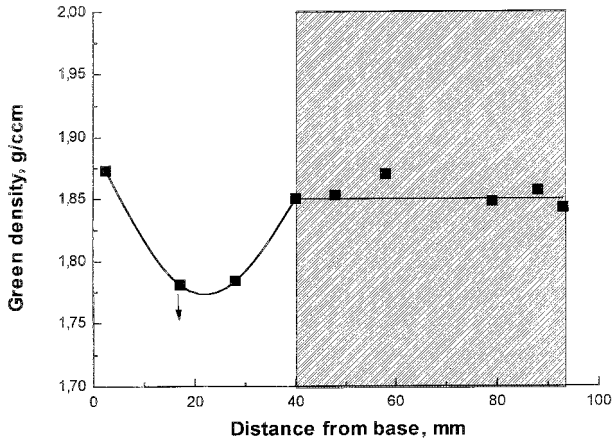


**Fig. 3.** Axial dependence of apparent green density in 0·6 GPa alumina compact. Cracked bottom half of compact is hatched.

region and loss of the shell's stability, with subsequent latent cracking in the bottom half. A closely packed layer at the flat base of the cylinder is absent. After breakdown of the shell the density equalizes.

Radial density distribution in the top half preserved integrity (at 17 mm from the top base, see Fig. 3) is presented in Fig. 4. Since the surface layer partially separates during crushing along clearly distinguishable cylindrical interfaces, it was possible to measure its thickness directly. It is shown in Fig. 4 as a hatched region.

As it can be seen, the density of the surface cylindrical layer is well approximated by precalculated close packing density (Table 1) and thickness of the layer coincides with the value predicted from eqn (1). Local central maximum is probably related to density redistribution in the bottom half after breakdown of the shell.

Buckle number $n$ for the given geometry is estimated from eqn (4) to be about 3. Consequently, the number of radial cracks equal to $2n$ must be about 6, and mean block size $2\pi R/6$ must be about 30 mm. This prediction completely corresponds to observations.

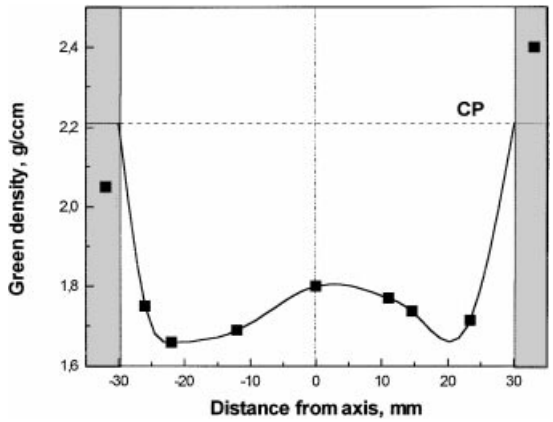


**Fig. 4.** Radial dependence of apparent green density in 0·6 GPa alumina compact. Calculated level of close packing (CP) and thickness of surface layer are shown too.

## 4 Discussion and Conclusions

It follows from the obtained results that arch effect disappears at some critical pressure close to yield stress of the material. On the other hand, it would hardly be possible at buckle number $n < 2$. One can easily derive from eqn (4) that the last superimposes a condition [again substituting eqn (1)]

$$\frac{R}{L} \geqslant 0{\cdot}194 \tag{7}$$

on $R/L$ ratio for the cylinder or given cylindrical section. In other words, long cylindrical rods are quite strong against crushing by external pressure.

Using eqns (3) and (6), and yield criterion we can build now an 'arch effect diagram' similar to the one demonstrated in Fig. 5. Here low pressure range (blank) responds to simple arch effect which involves some problems only during green drilling. Middle pressure range (hatched) presents latent cracking of cylindrical compacts that is extremely undesirable in both green machining and sintering. High pressure range (cross-hatched) beyond the yield criterion allows the production of homogeneous close-packed compacts without arch effect, suitable for machining as well as sintering, but very sensitive to recrystallization during sintering.

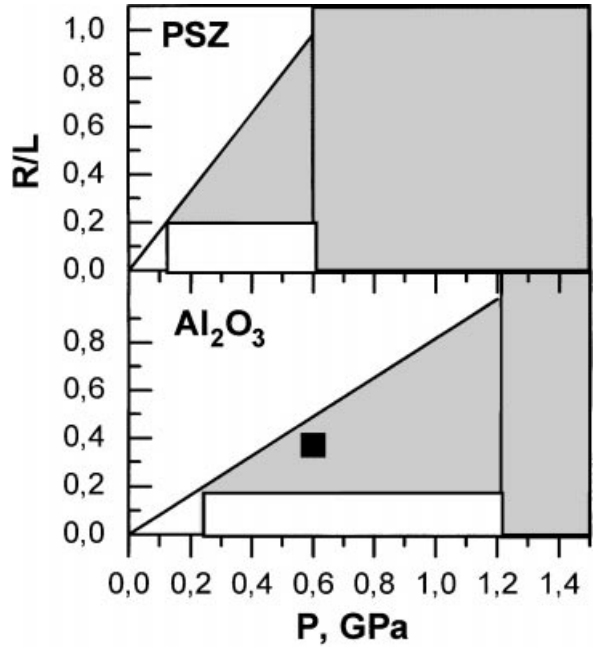


**Fig. 5.** Arch effect diagram derived from eqns (3) and (6), and yield criteria for PSZ and alumina cylindrical compacts. Filled point corresponds to conditions of the present experiment.

It is worth noting that yield criterion is reached locally at the powder particles contacts much earlier than overall yielding condition because of higher local contact pressure. However, it has only a little relation to blurring out the force lines unlike the general yield criteria.

The only experimental point in Fig. 5 relates to the above described 0·6 GPa alumina experiment. It is seen that the point strikes down into a latent cracking range very close to its border. This explains why the pressing has been cracked in the bottom part only. Maybe that half was the first one which met a pressure wave from a piston. Subsequent cracking had equalized density in it and made the remaining half of the cylinder shorter, displacing it over the upper border in the diagram.

Some general comments about the diagram may also be made. Firstly, every cylindrical ware intended to be manufactured using CIP, must be precalculated in the described manner as for optimum CIP pressure in order to preclude the latent cracking. Secondly, most unfavourable in view of the arch effect are the cylindrical ware with $R/L$ from 0·2 to 0·5 while long rods as well as flat disks are probably quite arch proof. Typical examples can be ceramic ball valves, endoprostetics etc. Thirdly, physically optimum CIP pressures are generally quite high and lie beyond yield stress for chosen material; in such cases the conditions of sintering must be considerably softened. Much more frequently used low CIP pressures are safe enough at $p \leqslant 0{\cdot}001E$ as accounted from eqns (3) and (6). For PSZ this safe pressure range is limited by 0·14 GPa and for alumina 0·28 GPa.

## References


1. Kiparisov, S. S. and Libenson, G. A., *Powder Metallurgy*, Metallurgiya, Moscow, 1971.
2. *Isostatic Pressing Technology*, ed. P. J. James. Appl. Sci. Publ., London, NY, 1989, p. 193.
3. Prokhorov, I. Yu. and Akimov, G. Ya., Cold isostatic pressing as a method of preforming green ceramic ware. *J. Eur. Ceram. Soc.*, 1997, **17**, 129–131.
4. Takashi, I., Yoshimoto, W. and Hiroshi, S., Simulation of random packing processes of the powder with forsfield's size distribution and analysis of the packing configuration. *J. Jap. Inst. Metals*, 1986, **50**(4), 423–429 (in Japanese).
5. Norio, O. and Tatsuo, T, Contact number and porosity in random packing of various sized spheres. *Powder Technol.*: Pap. Int. Symp., Kyoto, 28 Sept–1 Oct., 1981, Washington, e.a., 1984, p. 110–117.
6. Nikolenko, A. N. and Kovalchenko, M. S., Analysis of random packing of identical particles. II. Structural features of packing disks in the plane. *Powder Metallurgy (Rus.)*, 1985, **12**, 38–40 (in Russian).
7. *Strength, Stability, Vibrations: Handbook*, ed. I. A. Birger and Ya. G. Panovko. Vol. 3. Mashinostroyeniye, Moscow, 1968.
8. Stepanov, T. V. and Zubov, V. I., Elastic compression of porous metals. *Problems of Strength (Ukr.)*, 1986, **6**, 36–40 (in Russian).
9. Phillips, R. R. and Franciscovich, W., Free–free resonant frequency testing of powder metal alloys to determine elastic moduli. *Annu. Powder Met. Conf.: Proc. New Orleans*, L.A., 1–4, May, 1981, Princeton, NJ, 1984, 369–390.
10. Coble, R. L. and Parikh, N. M., Fracture of polycrystalline ceramics. In *Fracture*. ed. G.Libovits. Vol. 7, Pt 1.
11. Gogotsi, G. A., Mechanical features of a new structural material—zirconia crystals. *Fracture Mechanics and Physics of Brittle Materials: Ann. Inst. Mater. Sci. Probl. Kiev*, 1992, 33–41 (in Russian).
12. Castaing, J., Cadoz, L. and Philibert, J., Déformation plastique de l'alumine mono- et polycrystalline entre 200 et 1800°C. *Rev. int. hautes temp. et refract*, 1982, **19**(4), 337–380.
13. Chaika, E. V., Timchenko, V. M. and Akimov, G.Ya, Green machining of compacts obtained using cold isostatic pressing. *High Pressure Physics and Technology (Ukraine)*, 1998, **8**(3), 126–130.